MSA UNIVERSITY ENGINEERING JOURNAL

Efficiency of (GFRP- Steel) Stirrups in Reinforcing the Punching of Slab-Column Connections subjected to Eccentric Load

Mohamed H. Makhlouf [a], Gamal Ismail [b], Ahmed H. Abdel Kareem [c], Marwa I. Badawi [d*]

[a] *Associate Prof. in Civil Engineering Department, Benha Faculty of Engineering, Benha University, Benha, Egypt*

[b] *Professor in Civil Engineering Department, Benha Faculty of Engineering, Benha University, Benha, Egypt*

[c] *Professor in Civil Engineering Department Benha Faculty of Engineering, Benha University, Benha, Egypt*

[d*] *Teaching Assistant in Civil Engineering Department Benha Faculty of Engineering, Benha University, Benha, Egypt*

Abstract

The effectiveness of inner stirrups as the punching shear reinforcement for slab-column connections under eccentric loading was studied in this research with the purpose of improving the punching behaviour. This research experimental data and results study the effect of using steel, and glass fiber reinforced polymer stirrups (GFRPS) as punching shear reinforcement for interior slab-column connections (S-C-C) under eccentric loading. The experimental program consists of six flat slabs with dimensions of 1600*1600 *150 mm, stub column having a 200*200 mm cross-section with 700 mm total height extended outside both sides of the slab. The variables were the materials used for manufacturing stirrups (Steel - GFRP), the distance between stirrups (50 or 70) mm, and the case of loading (eccentric or centric load). The experimental results showed a noticeable increase in punching shear resistance for the slabs reinforced with stirrups ranged from 28 to 63% compared to the control specimen. Finite element analysis was performed using the Abaqus/CAE6.14 software, and the results were compared to the experimental results, which revealed a significant agreement. A Parametric analysis

ENGINEERING JOURNAL Volume 2 Issue 2
Accepted Date March 2023
Published Date March 2023
DOI: 10.21608/MSAENG.2023.291903

DOI:10.4186/ej.2009.VOL.ISSUE.pp

was also performed on the validated model. Finally, Equations for punching strength prediction were applied and then compared with the experimental results.

Keywords: Punching-Shear-Stirrups, GFRPS, Eccentric, Abaqus, Parametric.

1. Introduction

Flat slabs (F-S) are among the most widely used systems in reinforced concrete (R-C) constructions. By utilizing the F-S system, architects have more freedom in terms of building height, and more straightforward architectural modification after construction [1]. Practically all technologically advanced forms of reinforced concrete use frame structures of the slab-column connection (S-C-C) type. Most often, construction techniques technologies require the use of F-S without heads. The primary issue related to the structure's safety in these objects is punching. Several papers and research have discussed the problem of S-C-C in R-C structures collapsed by punching [2]. Reinforcement methods have been tested over the past several years by researchers to stop F-S from collapsing suddenly under punching shear. Recently, much attention has been given to the reinforcement and strengthening of structural elements against shear and flexure using composite materials. FRP has become a wise substitute for conventional reinforcing techniques because of lower material prices, as well as time savings from its lightweight and high tensile strength, ease of installation, and corrosion resistance [3]. In general, many inventive researchers initially used FRP materials to strengthen structural parts [4-10]. FRP can be applied using either an internal or exterior fixation method. FRP sheets or laminates are attached to the tension face for the parts utilizing EPOXY resin in the externally strengthened approach. By delaying the formation of punching shear cracks, this approach has improved flexural reinforcement and hence punching strength for existing slabs [11]. Much research has been accomplished for improving the punching performance of existing flat slabs using FRP materials [2,12]. Khalil et al. tested four half-scale reinforced concrete S-S-C for verifying the effectiveness of applying FRPS techniques to strengthen S-S-C subjected to punching shear [13]. Reinforced concrete F-S subjected to eccentric punching loads was studied by more few researchers [14-16]. The slabs were subjected to failure under association of axial load and unbalanced moment in order to determine the effectiveness of GFRPS for punching reinforcement in edge S-S-C strengthened with GFRP bars [17]. Numerous connection types were proposed, including shear bands made of steel beams I shape to improve punching shear strength and stability of connections among slab-CFT columns based on a known sensitive connection among column and R-C slab [18-19]. Most previous investigations have concentrated on the behaviour of F-S that are just flexural reinforced by GFRP bars. Additionally, corrugated GFRP links could be used as FRP-shear reinforcement to enhance the punching shear [20-21]. According to studies on S-C-C reinforced with GFRP bars, Mostafa et al. investigated 2 kinds of GFRP punching reinforcement, including GFRP studs and curved GFRP bars. According to the test results, two types of shear reinforcement could effectively avoid brittle punching- failure near the column. In comparison to those without shear reinforcement, shear studs and curved GFRP rods had average improvements for ultimate shear capacity of 27 and 16% and deformation of 64 and 46%, respectively [22-23]. Furthermore, FRP reinforced concrete (FRP-R-C) was expanding globally as a practical choice to traditional R-C by steel, which was being studied by some researchers [24-25]. Deifalla created a mechanical model based on punching performance for FRP-R-C slabs. Massive experimental data contained FRP-R-C slabs collected from a lot of researches. A novel mechanical model was discovered and offered in accordance with the critical shear crack theory (CSCT). The behaviour of the model, which was based on a physical model, was accurately observed. The suggested model takes into account the numerous failure mechanisms as well as the impact of Young's modulus. It is able to predict the rigidity and rotation of FRP-R-C slabs when subjected to punching load [26].

Steel stirrups were used as punching reinforcement to improve the punching behaviour for flat slabs, but FRPS were used slightly in the literature, also, those used for strengthening existing slabs. But may be applying FRPS as transverse reinforcement within F-S falls under the internal reinforced method for S-C-C. This research aims to study punching shear reinforcement by unconventional materials in F-S subjected to eccentric load and check its efficiency by comparing it with the code requirements. punching strength of S-C-C in F-S under eccentric loading was evaluated in this research. Punching strength of R-C-F-S subjected to eccentric load was studied when it was reinforced with (steel-GFRP) stirrups as punching shear reinforcement, which were rarely found in the literature which used punching shear reinforcement. Finite element analysis using Abaqus/CAE6.14 software was applied, and the outcomes were compared to those of the experimental results. In addition, Parametric analysis was performed on the validated model.

2. Experimental Procedure

2.1. Specimens

The test program consists of six F-S-C-Cs subjected to eccentric load specimens (see Table 1). The purpose of this study is to investigate shear reinforcement in F-S subjected to eccentric load by different materials and check its efficiency. The punching shear strength of S-C-C in an F-S system subjected to eccentric load was studied in order to improve this strength by using different materials. So various kinds of materials will be utilized in the reinforcement, and the distance between stirrups will be different. Six half-scale slabs were built and examined in the experimental program. Divided into control (co), one specimen subjected to eccentric load, one specimen subjected to centric load, and two groups reinforced with stirrups as punching reinforcement manufactured from different materials. Each specimen consists of an R-C slab with a cross-section of 1600*1600 mm and a thickness of 150 mm. The Column of (a 200x200) mm cross-section, 400 mm height from the upper and 150 mm from the lower. The first group consists of two slab specimens reinforced with steel stirrups with 140 mm width and the distances between each other were variable. The second group consists of two slab specimens reinforced with GFRPS with 140 mm width and the distances between each other were variable. Figs. 1, 2 indicate reinforcing schemes applied in the current research.

The reinforcement utilized is high-tensile steel (40/52). The slab is reinforced with a top mesh of 10 mm diameter, and a bottom mesh of 12 mm diameter. The lower mesh was 13Ø12 and the upper mesh was 13Ø10. Vertical high tensile steel bars 5Ø16 were used to reinforce the columns in the tension side and 2Ø16 in the opposite side of the column, with steel stirrups of 10 mm every 100 mm. At the upper and lower surface of the slabs, a clear concrete cover of 20 mm was maintained.

The variables of the test program are the following:

1. The materials used in the transverse reinforcement: Steel, and GFRPS.
2. The distance between stirrups: 50 mm or 70 mm.

Table 1. Experimental program.

Group No.	Slab Code	Load Condition	Punching Shear Rft.		
			Applied Material	Distance Between Stirrups (mm)	Width of Stirrups (mm)
Reference	S1	Eccentric	-	-	-
	S2	Centric	-	-	-
1st. Group	S3	Eccentric	Steel	50	140
	S4			70	140
2nd. Group	S5		GFRPS	50	140
	S6			70	140

-All stirrups used as punching shear reinforcement = 8mm diameter, began at distance of 30 mm. The eccentric load at 60 mm from the centre of the column.

2.2. Materials Properties

2.2.1. Concrete

In the concrete mixtures of the experimental specimens, crushed dolomite with a maximum aggregate size of 16 mm, natural sand with fineness moduli of 2.7, and Ordinary Portland Cement (42.0 grade) were used. After 28 days, a compressive strength of 30 Mpa was required. On the testing day, cubes (150x150x150 mm) were formed and allowed to cure alongside the test specimens to achieve the true f_{cu}.

2.2.2. Steel bars

High tensile steel bars grade 52 were used as lower reinforcement (tension reinforcement) of the tested specimens, where their diameters were 12 mm, and bars of 10 mm diameters were utilized in upper reinforcement (compression side). Stirrups with 8 mm diameter bars were manufactured out of standard mild steel grade 40. An experimental test was carried out to estimate elongation, yield stress, ultimate stress, and Modulus of elasticity for the used steel. The mechanical properties of the steel bars (see Table 2).

2.2.3. GFRPS

GFRPS used in this research were manufactured from GFRPs strings (see Fig. 3a). The stirrups were added to the reinforcement as punching reinforcement. The stirrups used were made from GFRP strings collected and bonded using epoxy Sikadur-330 then put in a model, and a resin was cast and let till hardened. According to the manufacturer, Table 3 lists the mechanical characteristics of the GFRPS of 8 mm in diameter.

Table 2. Mechanical properties of steel reinforcement.

Steel Type	Yield Stress (MPa)	Tensile Strength (MPa)	Elongation %	Modulus of Elasticity (MPa)
High Tensile	410	526	16	210000
Normal Mild	256	405	24	204000

Table 3. Properties of GFRPS.

Characteristics	GFRPS
Dimensions (mm)	Diameter (8)
Tensile strength (Mpa)	1005
Elasticity modulus (Mpa)	53500
failure Strain %	1.88%

2.3. Reinforcement Technique with Stirrups

The GFRPS and steel stirrups were internally placed in the places of punching shear reinforcement with considered the ACI recommendations [27-29], (see Fig. 2, and Fig. 4 (c-d)). Then the specimens were cast and curried. The stirrups had a 140 mm width and were spaced apart by 50 or 70 mm.

2.4. Test Setup and Instrumentation

The specimens were suspended in a rigid reaction frame with a 1000 KN maximum capacity and subjected to eccentric or centric loads utilizing a hydraulic jack with that capacity. Which was attached to an electric pump. To act almost like simply supported, the four sides of the specimens were supported by steel beams. The I-shaped steel beams and rod bars were joined by welding. A thick metal plate was used to redistribute the load to the top of the column stub. Under the hydraulic jack, a load cell with a maximum capacity of 1000 KN was installed to record the applied load. Five LVDT (Linear Variable Differential Transducers) have been fixed below the centre of the column stub, and below eccentric load and at the quarter-span of the slab were applied to measure the displacement. Two strain gauges were installed on the stirrups and the concrete surface of each specimen. The cracks spread gradually as the load being applied increased till failure. Each test result was recorded on a computer for periods of two seconds utilizing a data acquisition system. Fig. 4 shows the specimen's reinforcement and punching shear reinforcement with stirrups. Fig. 5 demonstrates the test setup. The test set-up was applied in the concrete laboratory of the Benha Faculty of Engineering at Benha University.

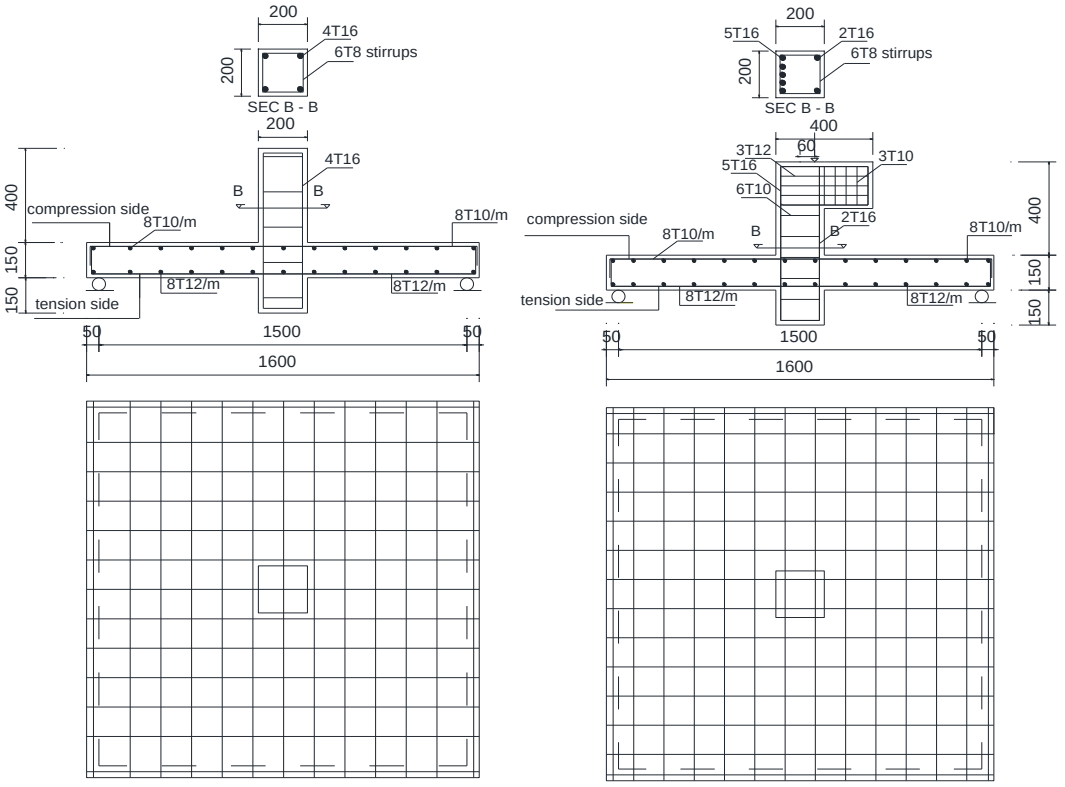

Fig. 1. Reinforcing schemes, a) Control under centric load, b) Control eccentric load. (All dimensions in mm)

3. Experimental Results and Discussions

The results of the experimental test are mentioned in Table 4. The next sections will investigate how test variables affected on tested specimens' performance subjected to punching load.

3.1. Load-Deflection Relationships

Figures 6–9 demonstrate the deflection (def) beneath the load effect on the F-S against the applied load corresponding to the test variables. The reference specimen's curve almost raised linearly until the ultimate load, at which point the load decreased abruptly because of brittle punching failure. All other specimens' load-def curves matched the reference curve, with the exception that the decrease in load after achieving its highest was less sharp and the displacement decreased with some elasticity. When compared to the reference specimen (0% punching shear reinforcement), the load-def curve indicates an increase in ultimate load and a lesser def at the same load in all other specimens with punching shear reinforcement. The def at the first crack and at the ultimate load was measured. The reduction in def of the reinforced specimens in comparison to the reference specimen was determined by evaluating the def of the test specimens just at the ultimate load of the reference specimen (Δuc) (see Table 4).

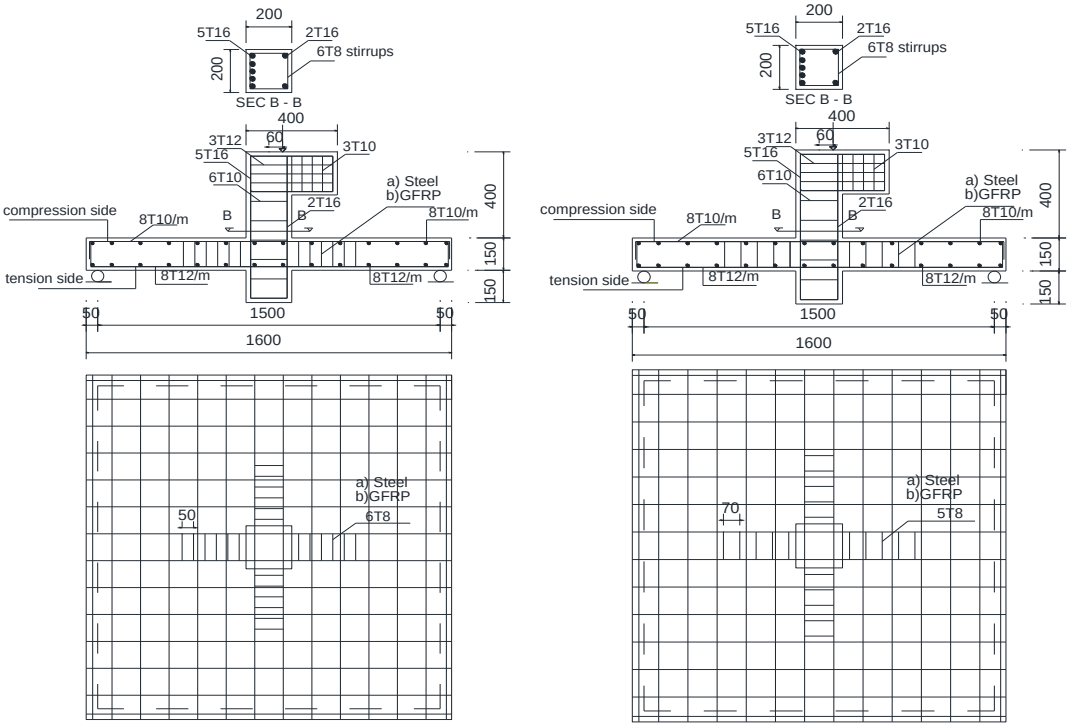

Fig. 2. Reinforcing schemes (all dimensions in mm): a) Steel Stirrups, b) GFRPS.

i) Stirrup's distance 50mm

ii) Stirrup's distance 70mm.


a)


b)

Fig. 3. FRPs a) GFRP strings, b) GFRPS stirrups.

a) Control under centric load.

b) Control under eccentric load.

c) Distance between stirrups 50mm.

d) Distance between stirrups 70mm.

Fig. 4. Reinforcement schemes.

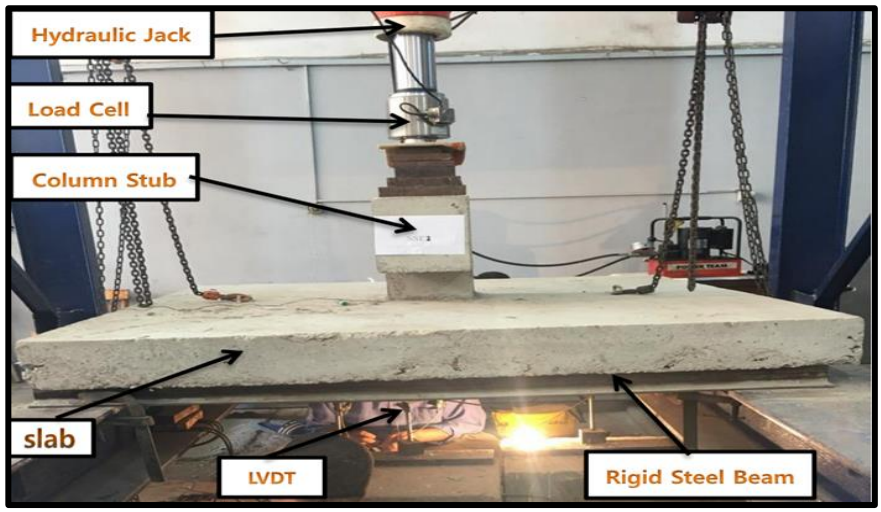

Fig. 5. Test Set-up.

3.1.1. Influence of distance between stirrups

Figures 6 and 7 showed the load-def relationship for steel and GFRPS with distance 50 and 70 mm between each other. Figure 6 showed two specimens reinforced by steel stirrups as punching reinforcement. Figure 7 showed two specimens reinforced with GFRPS as punching reinforcement. As the distance between steel stirrups decreased from 70 to 50 mm (reinforcement ratio increased) the maximum def increased from 13.86% to 30.83% compared to the reference specimen (0% punching shear reinforcement. When the distance among GFRPS decreased from 70 to 50 mm (reinforcement ratio increased) the maximum def increased from 11.03% to 27.3% compared to the control specimen.

3.1.2. Effect of using different materials in punching reinforcement (steel, and GFRPs)

Figure 8 (a, b) showed the load-def relationship for steel, and GFRPS with 140 mm width. Figure 8 (a) showed that the load-def relationship for GFRPs, and steel stirrups with distance 50 mm between each other, the maximum def increased from 27.3% to 30.83% respectively, compared to the control specimen. Figure 8 (b) showed two specimens reinforced with GFRPS and steel stirrups as punching reinforcement with distance 70 mm between each other, the maximum def increased from 11.03% to 13.86% respectively, compared to the control specimen. Thus, the specimens reinforced with steel stirrups showed a slight improvement in the ultimate def compared to the specimens reinforced with GFRPS. In comparison, GFRPS were preferred over steel stirrups due to their higher shear capacity and anti-corrosion.

3.1.3. Effect of the load case (centric - eccentric)

Figure 9 showed the load-def relationship between two specimens without punching shear reinforcement (stirrups) subjected to different load cases. The maximum def for specimens subjected to centric load increased by 8.6% compared to the specimens subjected to eccentric load (reference specimen).

3.2. Load Carrying Capacity

Table 4 illustrates the load at the first crack (Pcr), the ultimate load (Pu), and the improvement in Pu for the reinforced specimens over the control specimen. When compared to the control specimen, specimens reinforced with GFRP, or steel stirrups improved Pcr from 7.7% to 13.85%. Moreover, the ultimate load capacities of all reinforced specimens had significantly increased. Pu increased by 28.06% and 41.21% for specimens reinforced by steel stirrups of 140 mm width with 70 and 50 mm, respectively. The Pu increase for the specimens reinforced with GFRPS of 140 mm width with the distance of 70 and 50 mm was 42.48% and 62.56%, respectively, over the control specimen. Similarly, the improvement in Pu for centric load specimens over control specimens was 16.25%. While increasing the punching reinforcement ratio (reducing distance among stirrups from 70 to 50 mm) increased Pu by 10.26% and 14.1% for specimens reinforced by steel and GFRPS, respectively. As a result, we can conclude that using GFRPS caused a considerable increase in Pu when compared to using steel stirrups, while reinforced specimens against punching shear caused a substantial increase in Pu when compared to control specimens, (see Figs. 6, and Figs. 7).

According to the load case, the specimens subjected to centric load showed a relatively higher increase in Pu than the specimens subjected to eccentric load (see Fig. 9, and Figs. 12). The punching shear capacity of all specimens increases as the distance between stirrups decreases (see Figs. 8 (a-b), and Figs.11).

3.3. Stiffness

The initial stiffness (Ki) at the uncracked stage and the ultimate stiffness (Ku) were shown in Table 4, which is estimated for all the tested specimens from the load quantities and the def at the cracking and ultimate case. It showed that ki increased significantly for reinforced specimens by 31.88-56.4% for specimens reinforced with steel stirrups and 41.88-45.65% for specimens reinforced with GFRPS while increasing the distance between stirrups from 50 to 70 mm respectively in comparison to control specimen. Furthermore, using punching shear reinforcement affected the ultimate stiffness (Ku) value. Where Ku had a notable increase for specimens reinforced with GFRPs by 24.5-25.6%, and a significant increase for specimens reinforced with steel stirrups by 13.92-17.78% in comparison to the control specimen. A relative increase for specimens subjected to centric load by 10.37% in comparison to the control specimens (subjected to eccentric load).

Considering the effect of punching shear reinforcement, the reinforced specimens demonstrated better stiffness in comparison to the control specimen. The results showed that Ki was more influenced by punching shear reinforcement than Ku for specimens reinforced with GFRPS, while Ku was less affected by punching shear reinforcement than Ki for specimens reinforced with steel stirrups.

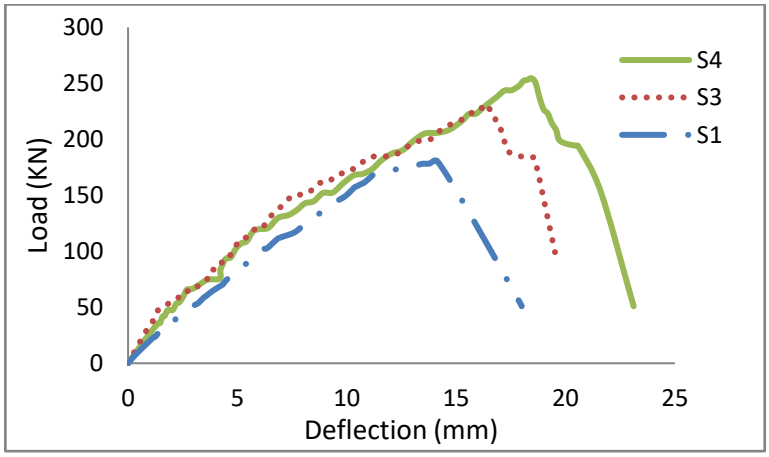

Fig. 6. Load- Def comparison depended on the distance between steel stirrups.

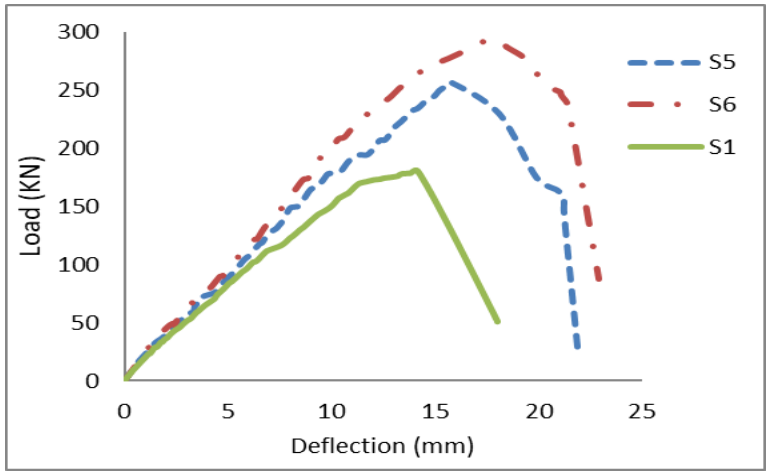

Fig. 7. Load- Def comparison depended on the distance between GFRPs.

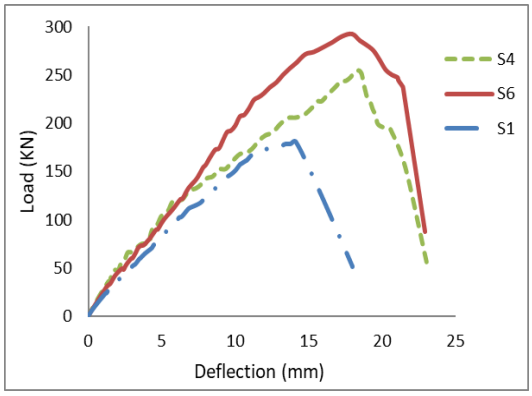

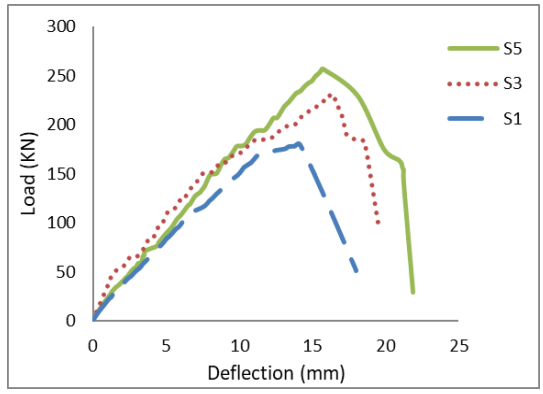

a) Stirrup's distance 50mm. b) Stirrup's distance 70mm.

Fig. 8. Load- Def comparison depended on type of punching reinforcement material.

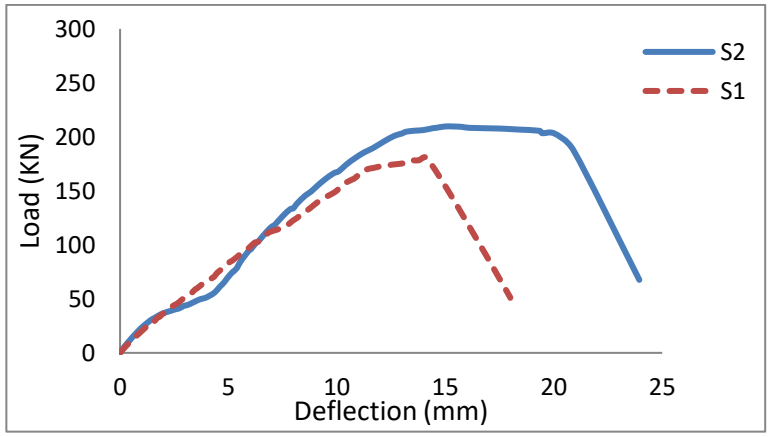

Fig. 9. Load- Def comparison depended on load case (centric-eccentric).

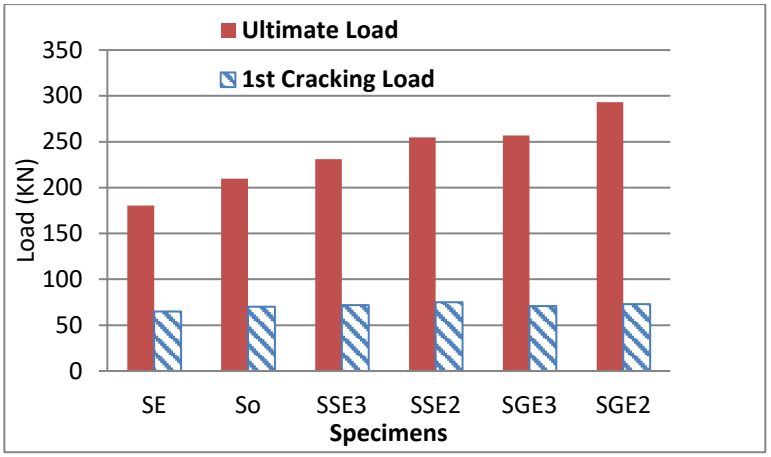

Fig. 10. comparison between 1st cracking load and ultimate load.

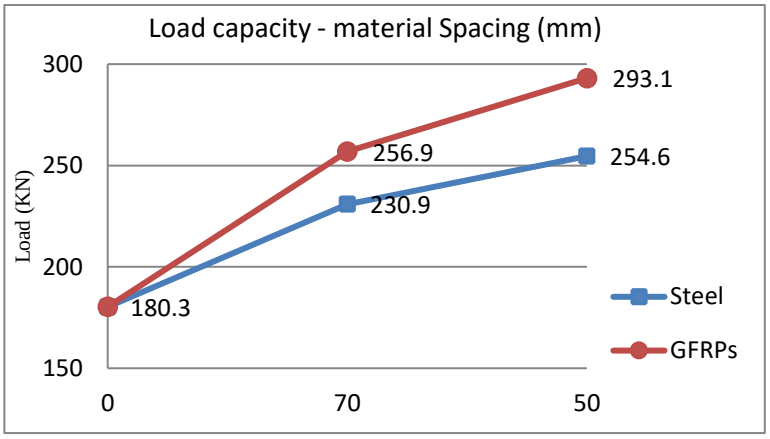

Fig. 11. Load carrying capacity- different materials with different distance.

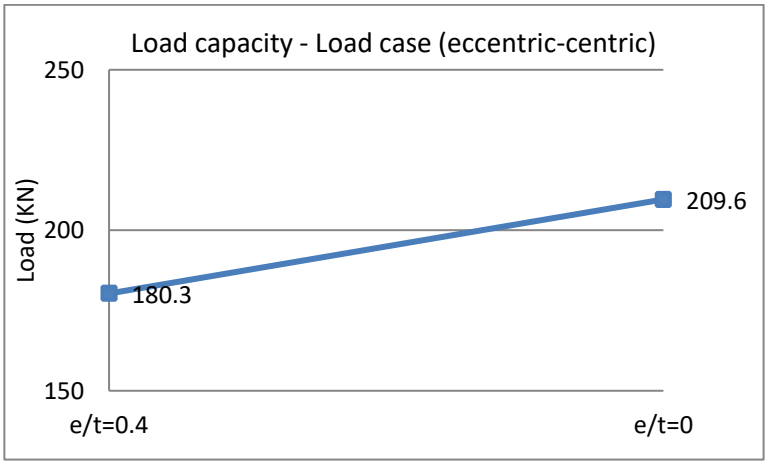

Fig. 12. Load- Def comparison depended on the distance between GFRPs.

3.4. Strain

The strain at about d/2 from column face (on the stirrup at d/2 from the column face) of R-C slabs were illustrated by load-strain curves. From the load- strain curves, strain ductility (μs) was identified as the ratio between strain at ultimate load to the strain at the yielding load (μs=εu/εy) [27]. Table 4 shows the strain in stirrups of all specimens at the ultimate load (Pu), yield load (Py), and strain ductility (μs).

The strain ductility for all specimens reinforced with (steel, and GFRPs) increased with the increasing of punching reinforcement ratio due to the better load-carrying capacities of specimens as indicated in the load-strain curves (see Figs. 13-15). As the punching shear reinforcement ratio (70, 50mm distance) increased the strain ductility increased and this value was 6.5% for steel stirrups, and 12.77% for GFRPS. The specimens reinforced with punching reinforcement manufactured from GFRPs enhanced the strain ductility than the tested specimens reinforced with punching reinforcement manufactured from steel by approximately 21.37% for stirrups with 50 mm distance, while enhanced the strain ductility of the tested specimens by approximately 14.63% for stirrups with 70 mm distance. According to the results of the experimental test, the ultimate strains of specimens reinforced by steel stirrups were lower than those of specimens reinforced by GFRPS, and the development of strain also increased slowly. The strain ductility ratio of specimens reinforced with GFRPS was greater than specimens reinforced with steel stirrups.

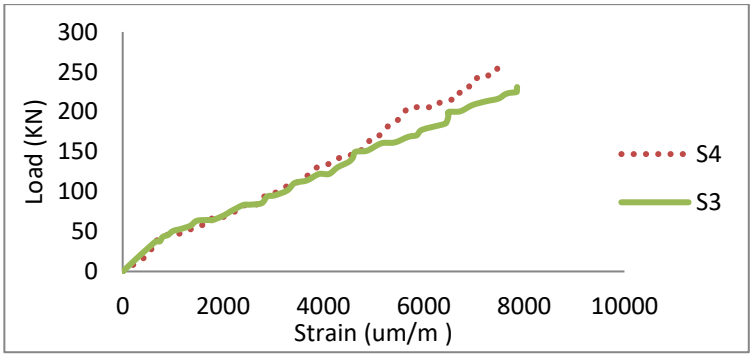

Fig. 13. Load- Strain comparison depended on the distance between steel stirrups.

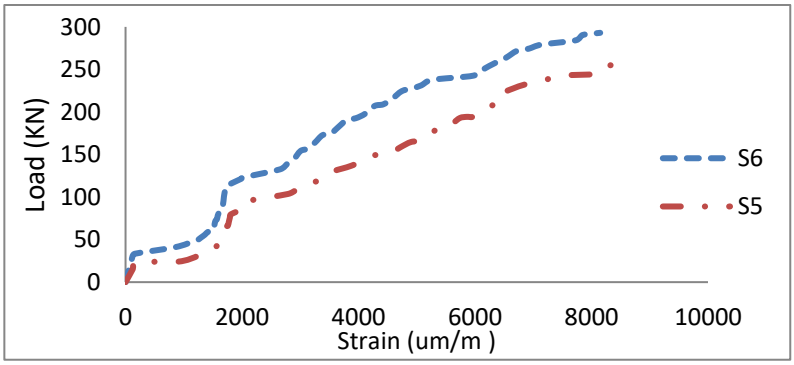

Fig. 14. Load- Strain comparison depended on the distance between GFRPS.

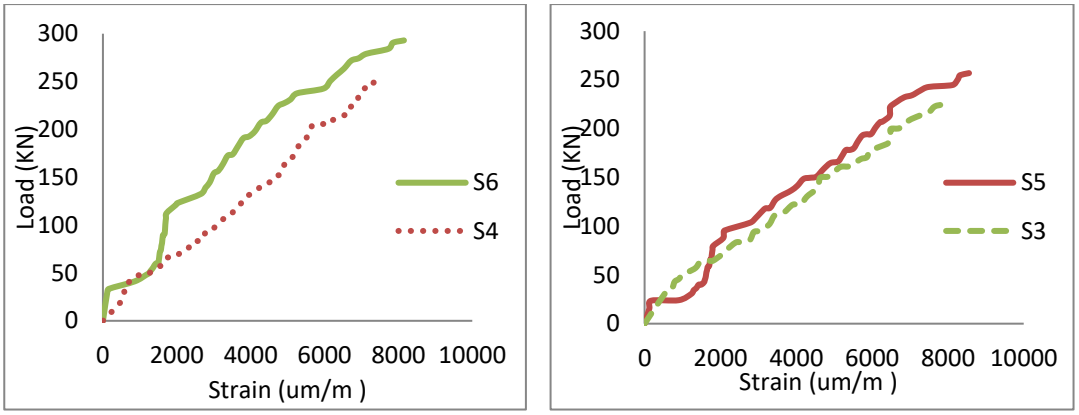

a) Stirrup's distance 50mm. b) Stirrup's distance 70mm.

Fig. 15. Load- Strain comparison depended on type of punching reinforcement material.

3.5. Crack patterns and failure characteristics

Figure 16 displays the pattern of cracking propagation and distribution during failure at the lower side of the F-S specimens for all examined samples. All specimens collapsed by punching shear as the mode of failure. Control specimen demonstrated according to punching shear loads, while some flexural cracks started close to column stub and expanded in the direction of the F-S edges, mainly near the corners when the affected load grew. The F-S collapsed suddenly as they reached their maximum capacity, and the load applied to the specimen dropped suddenly as a result. Punching cracking caused separation from the slab surface and drew on the bottom side, which is visible clearly around the column and at widths ranging from 340 mm to the slab borders (650 mm) from its face.

The specimens reinforced with GFRPS failed without warning in punching shear by a brittle behaviour, no warning was observed, and large spallation of concrete cover at tension side was observed. While slight cracks were appeared in the compression side. Adding punching shear reinforcement stirrups not only changed the shape of punching failure plane but also shifted the failure plane away from the column face. Specimens subjected to eccentric load; the flexural cracks increased at the side of the applied load. The specimen subjected to centric load; The slab edges noticed the propagate of the flexural cracks. The punching strength of the specimen was raised by limiting the growth of flexural cracks in the area surrounding the columns. Distances from punching shear failure sections to column face were shorter in specimens reinforced by punching reinforcement than in control specimens.

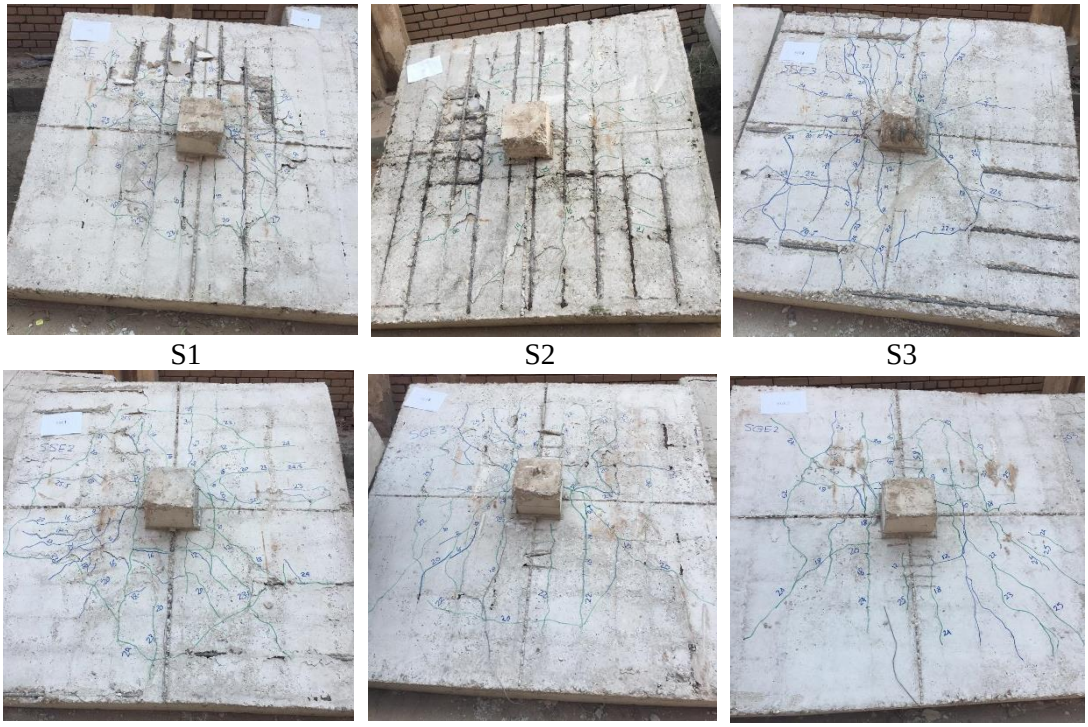

Fig. 16. crack pattern at failure (bottom face).

Table 4. Summary of experimental results.

Spec. ID	1st cracking		Ultimate			$\frac{Pu}{P\ co.}$	Δuc = $\frac{\Delta u * P\ co.}{pu}$	Un-cracked stiffness (Ki) $\frac{Pcr}{\Delta cr}$	Ultimate stiffness (Ku) $\frac{Pu-pcr}{\Delta u-\Delta cr}$	Yielding Level (y)		Strain Ductility, μs=εu/εy
	Load Pcr (KN)	Def Δcr (mm)	Load Pu (KN)	Def Δu (mm)	Strain (εu) (um/m)					Load (Py) (KN)	Strain (εy) (um/m)	
S1	65	4.8	180.3	14.1	-	1.00	14.1	13.54	12.34	144.3	-	-
S2	70	5.1	209.6	15.4	-	1.16	13.2	13.73	13.62	168	-	-
S3	72	3.4	230.9	16.1	7860	1.28	12.6	21.18	12.51	184.7	6404	1.23
S4	75	4.2	254.6	18.5	7467	1.41	13.1	17.86	12.56	203.7	5705	1.31
S5	71	3.6	256.9	15.7	8557	1.42	11.0	19.72	15.36	205.5	6050	1.41
S6	73	3.8	293.1	18.0	8149	1.63	11.07	19.21	15.50	234.5	5110	1.59

4. Theoretical Modelling

4.1. Flat slabs with punching shear reinforcement (steel)

Punching stress exhausted all specimens at the critical section, which was located (d/2) apart from the outer punching shear stirrup. Based on the expected ultimate loads of the tested specimens, the following equations can be proposed to calculate the values of punching shear strength (Vn), as shown in Eq. (1): [30].

$$v_n = \frac{(v_c + v_s)}{\beta} \quad (1)$$

$$v_c = 0.33\left[1 - \frac{\alpha - 1}{6}\right]\sqrt{f_c'} \qquad (Mpa) \quad (2)$$

Where:

V*c*: concrete shear resistance.
V*s*: reinforcement shear resistance.
β: factor depending on the eccentricity of the punching shear force and can be assumed equal to 1, 1.15 and 1.3 for e/t = 0, e/t < 0.5 and e/t >0.5 respectively. The values of β were proposed based on the experimental results obtained in this study.

α: ratio of critical section distance between column face and effective depth of slab 4≥α≥1.
fc': compressive strength of a concrete cylinder.

The following Eq. (3), and Eq. (4) can be used to determine the ultimate punching capacity at any critical section [14-15]:

$$v_c = v_c \,.\, b_o \,.\, d \quad (3)$$

v_c: provided by Eq. (2).

$$v_s = \frac{A_v \,.\, f_{yv} \,.\, d}{s} \quad (4)$$

Where:

bo: perimeter measured at d/2 from the farthest row of punching shear reinforcement.
d: effective depth of the slab.
Av: the area of the vertical legs that form the shear reinforcement units in a single row.
Fyv: yield stress for the steel of shear reinforcement.
S: the distance between rows.

There are currently no ACI 440.1R theories for estimating the ultimate punching capacity of reinforced concrete slabs with FRP punching reinforcement (stirrups). The

following design conditions are an extension to ACI 440.1R that considers FRP stirrups as punching reinforcement and their effects on the ultimate capacity of flat slab column connections reinforced with FRP punching reinforcement.

4.2. Flat Slabs with punching shear reinforcement (FRPs)

In accordance with ACI 440.1R, Eq. (7) for steel stirrups was modified to compute the FRPs-stirrups participation. The suggested design equations for FRP-reinforced specimens could be summarized as follows in Eq. (8). Suggested design conditions for punching shear-reinforcement:

$$v_c = \frac{2}{5}\, k\, \sqrt{f_c'} \qquad (Mpa) \qquad (5)$$

$$K = \sqrt{2\rho_f n_f + (\rho_f n_f)^2} - \rho_f n_f \qquad (6)$$

$$v_{fv} = \frac{\phi_f\, A_{fv}\, (0.004\, E_{fv})}{b_o S_{fv}} \qquad (\text{Mpa}) \qquad (7)$$

$$v_n = \frac{(v_c + v_{fv}).\ b_o .\ d}{\beta} \qquad (8)$$

Where:

K: provided by Eq. (6).
ρ_f: FRP reinforcement ratio.
n_f: number of stirrups rows.
ϕ_f: reduction factor depending on spacing between stirrups and material type.
E_f: FRP modulus of elasticity.
S: the distance between rows.

A comparison between the theoretical values of the ultimate load (Pu TH) and the corresponding experimental values (Pu EXP.) was indicated in Table 6, and Fig. 18.

5. Non-linear finite element analysis

5.1. General

In this research, the punching performance of an R-C-S-S-C was simulated by applying a nonlinear finite-element (FE) analysis utilizing the FE software Abaqus/CAE standard 6.14-2. Many factors had to be considered in the modelling, including element types, material properties, part assembly, meshing the parts, steps, interaction between parts, loading conditions, and supporting types [31].The following sections provide a brief description of the elements used in this study to model concrete, steel reinforcing bars, steel support, and punching shear reinforcement (steel and GFRPS), as well as the boundary conditions. Some researchers are using FE analysis to model the punching performance of reinforced concrete S-S-C [32].

5.2. Materials properties and element types Modelling

5.2.1. Materials Properties

To accurately represent the experimental study, the Abaqus program was given the identical material properties used in the experimental program for the concrete, steel bars, and GFRPS. A variety of factors, including compressive strength of concrete, steel yielding stress, steel tensile strength, GFRPs tensile strength, and elasticity modulus for reinforcement bars, had to be considered in the simulation.

5.2.2. Modelling Descriptions and Concrete-Reinforcement Boundary

To model the concrete S-S-C and the ending support, a 3D deformable solid part was inserted. To model the steel bars, steel stirrups, and GFRPS, 3D deformable wire elements were inserted. The reinforcement was simulated as an embedded element within a 3D solid part element of concrete. As longitudinal bars, three material types were inserted to simulate reinforcement steel, GFRP, and CFRP. The slab-column connection was modelled at full scale. As shown in Fig. 17, the assembly of the parts was also patterned to contain the flat slab geometry during loading.

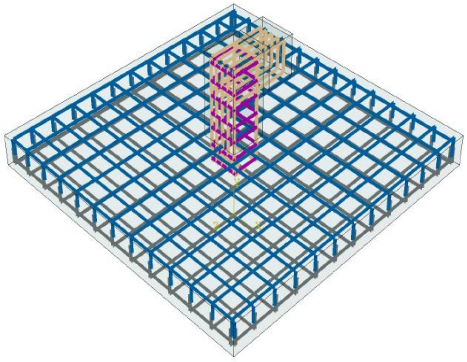

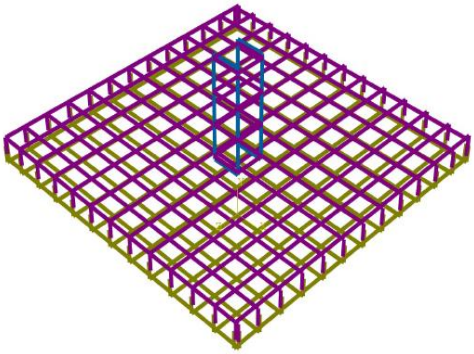

a) Reinforcing element with eccentric load (S1). b) Reinforcing element with centric load (S2).

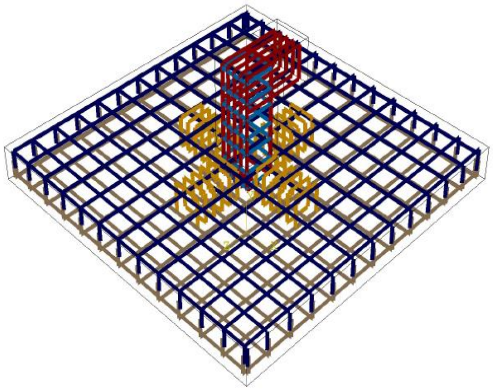

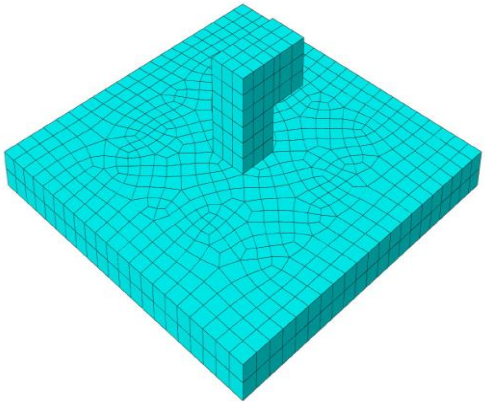

c)Reinforcing elements with stirrups. d) Mesh elements.

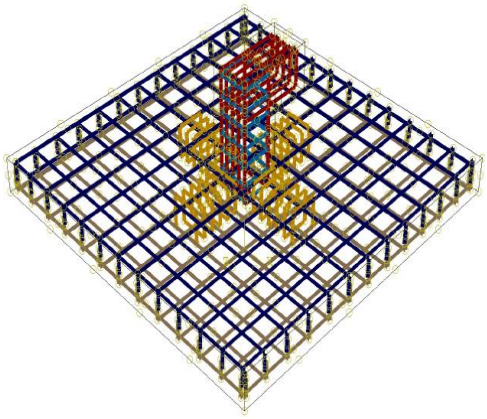

e) Embedded regions.

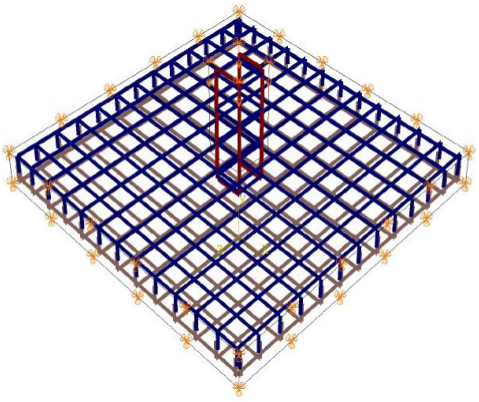

f) Load condition (centric load).

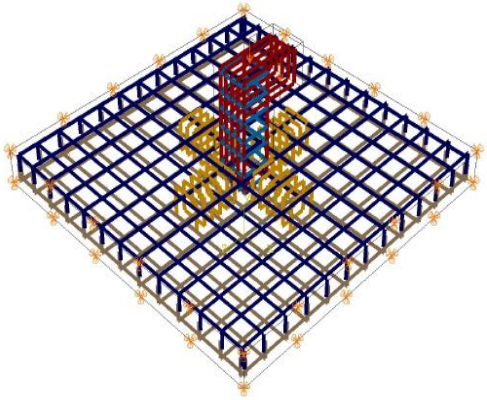

g) Load condition (eccentric load).

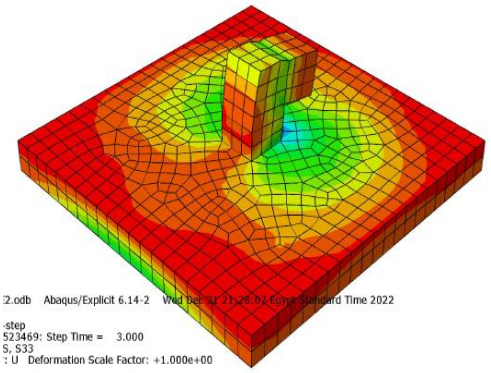

h) stresses.

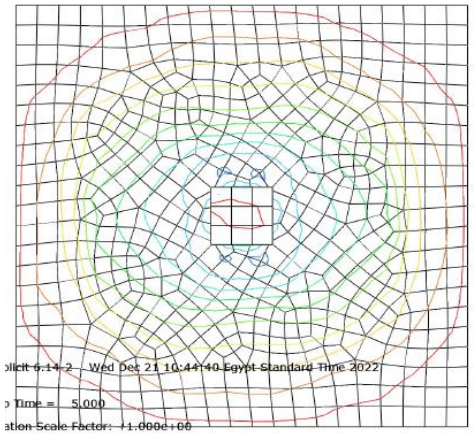

i) cracks pattern for specimen with centric load.

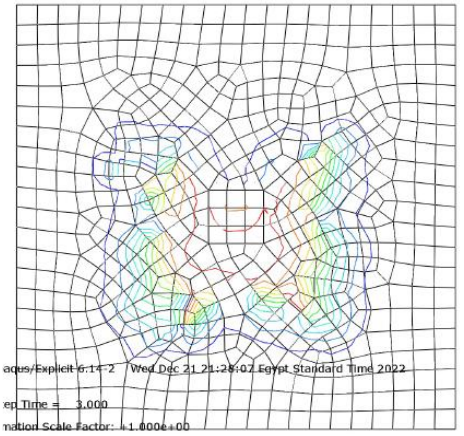

j) cracks pattern (eccentric load).

Fig. 17. Simulating of reinforcement concrete slab-column connections.

5.3. Solution Control

According to the nonlinear FE model established in the ABAQUS program may include several thousand variables, the entire load must be divided into a sequence of load steps to indicate the nonlinearity effect. One (KN) of the loads was applied at each step. In addition, at the end of each step, ABAQUS renews the solution and inserts it for the next step to account for nonlinearity. ABAQUS defined the solution as a series of slight increments, but after each increment is solved and the amount of the increment is chosen. As a numerical method to resolve the nonlinear equilibrium equations, Newton's method was chosen as the solver. The reason for this preference is initially Newton's method prediction accuracy compared to the convergence rates presented by different methods for the types of nonlinear difficulties most investigated with ABAQUS.

5.4. Experimental, and FEM results

The FEM simulation results were compared to the experimental results of the tested F-S specimens. The whole specimens were designed for the FE model verification procedure S1, S2, S3, S4, S5, and S6 achieved an improvement in ultimate load of 14.33%, 27.28%, 39.56%, 40%, and 59.49%, respectively, over the reference specimen (S1). Regarding the load-def curve, a comparison was made. The punching shear reinforcement ratio and the elastic modulus of the reinforcing bars were test parameters involved in the FE results. In FE modelling, such as that performed in the experimental program, steel and GFRP bars were used as reinforcing materials. The load-def curves of all specimens from experimental and FEM data are shown in Fig. 19, which also illustrates the influence of stirrup reinforcement on punching strength. The results demonstrated that FE models were capable to accurately reflect the load-def relationship of experimental results (see Fig. 19). In Fig. 18 as well as Table 6, experimental and FE results for ultimate loads were provided in reasonable agreement.

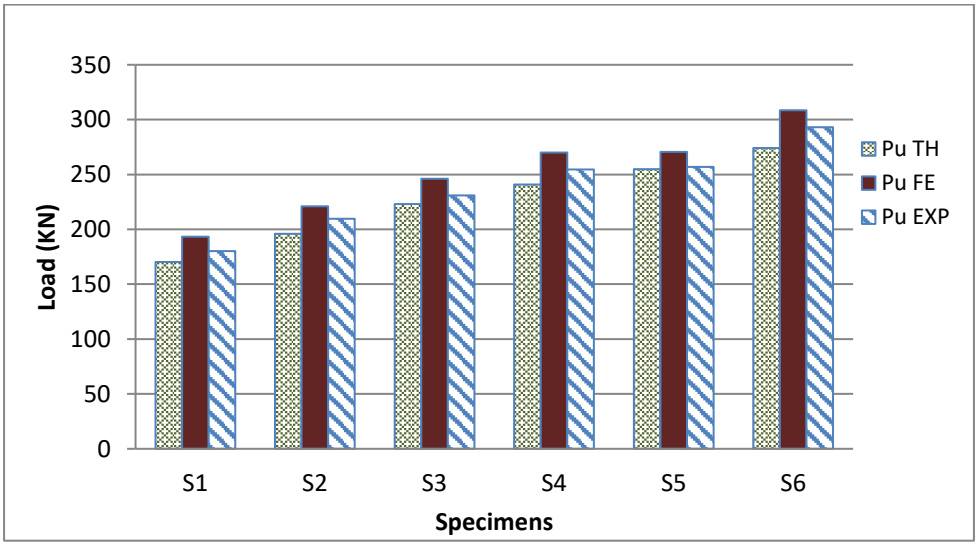

Fig. 18. Load- Def relationship by finite element analysis.

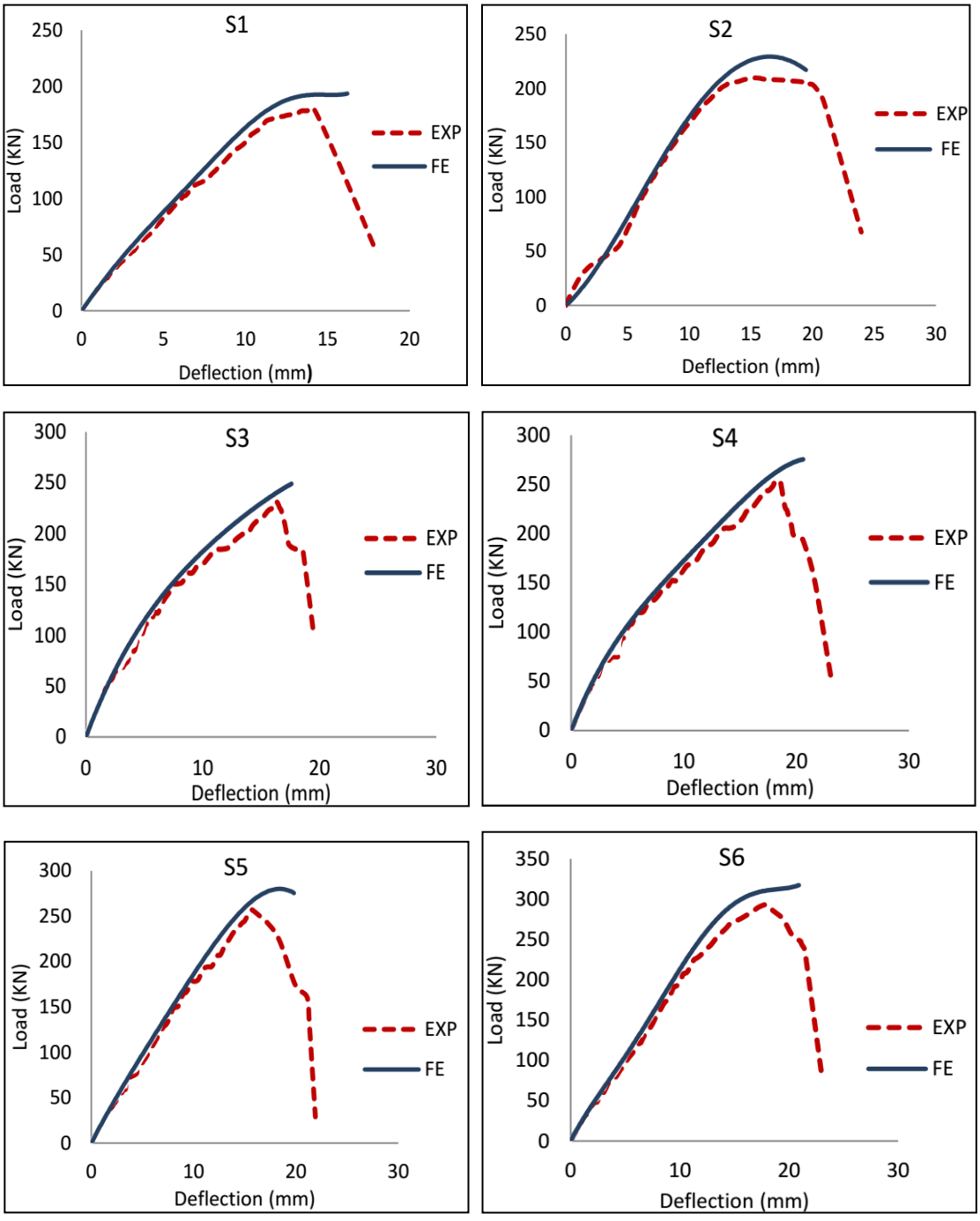

Fig. 19. Load- Def. relationship by finite element analysis.

Table 6. Comparison of Experimental, Theoretical, and FE Results.

Slab Code	Experimental Ult. load Pu EXP. (KN)	Theoretical Ult. load Pu TH. (KN)	Analytical Ult. Load Pu FE. (KN)	Pu TH/ Pu EXP	Pu FE/ Pu EXP
S1	180.3	170.3	193.4	0.94	1.073
S2	209.6	195.8	221.11	0.93	1.055
S3	230.9	223.1	246.15	0.97	1.066
S4	254.6	240.8	269.9	0.95	1.060
S5	256.9	255.0	270.63	0.99	1.053
S6	293.1	274.0	308.45	0.93	1.052
			Mean	0.95	1.058
			SD	0.024	0.008
			Covariance	0.0006	0.0001

6. Parametric Study

Utilizing the FE program Abaqus CAE6.14, a parametric analysis was performed to examine the effectiveness of inner stirrups as the punching reinforcement for S-S-C under eccentric load in addition to studying the effect of stirrups material types, distance, concrete compressive strength, and load case on slab connection. Three different material types were used which are CFRP, GFRP, and steel. Three different stirrups distances were used which are 30, 50, and 60 mm between each other. three different concrete compressive strengths were used which are Fcu=25,30, and 35 Mpa. three different load cases were used which are e/t =0 (centric load), e/t =0.4 (eccentric load), and e/t =0.8 (eccentric load), as indicated in (Figs 20 – 23), and table 7. Where the symbols were identified the specimens (S) as follows: steel (S), GFRP (G), CFRP (C), Distance =30 mm (1), Distance =50 mm (2), Distance =70 mm (3), Eccentric load (E), e/t = 0.4 (0.4), e/t = 0.8 (0.8), e/t = 0 (0), Fcu=25 Mpa (25), Fcu=30 Mpa (30), and Fcu=35 Mpa (35).

6.1. Effect of using stirrups with different material types (steel, CFRPs, and GFRPs)

The material types have a major influence on the FE-predicted punching capacities as shown in Fig. 20. As can be seen, with a change of the stirrups type there is also an increase in the FE punching load. Using CFRPS showed the best punching load capacity, then GFRPS. So, taking into consideration the cost of both, the use of GFRPS was preferred.

6.2. Effect of distance between punching shear reinforcement (60, 50, and 30mm)

The distance between stirrups expresses the punching reinforcement ratio. As the reinforcement ratio increased the distance between stirrups decreased. Fig. 21 indicated that by decreasing the distance between stirrups, there is an improvement in FE punching capacity. A distance of 30 mm presented the highest increment in the load-carrying capacity.

6.3. Effect of concrete compressive strength (Fcu)

Enhancing the concrete compressive strength results on an increment in the FE punching load as shown in Fig. 22. According to the characteristics of the concrete that represented in the Abaqus/CAE6.14. The FE punching load improved as concrete compressive strength increased.

6.4. Effect of eccentricity (e/t =0, e/t =0.4, and e/t =0.8)

The load position has a significant impact on the FE punching capacity as shown in Fig. 23. By increasing the eccentricity, the FE punching load was decreased. Using centric load e/t=0 presented the highest punching capacity and the best behaviour for the slab connection.

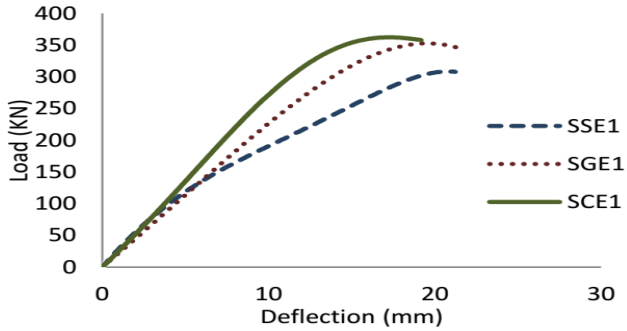

Fig. 20. Load- Def relationship by finite element analysis.

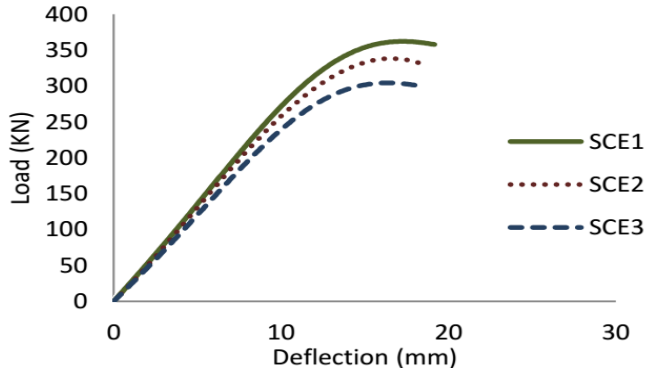

Fig. 21. Load- Def comparison depended on the distance between stirrups.

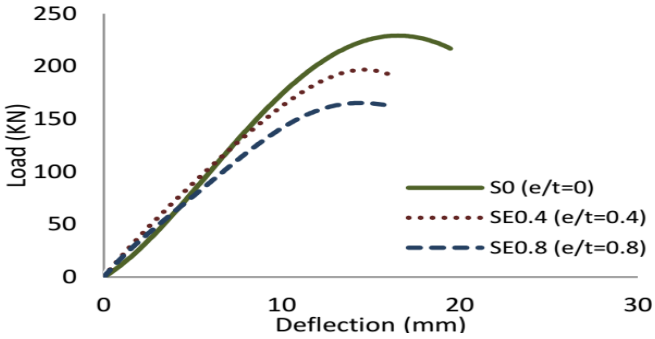

Fig. 22. Load- Def comparison depended on load case (centric-eccentric).

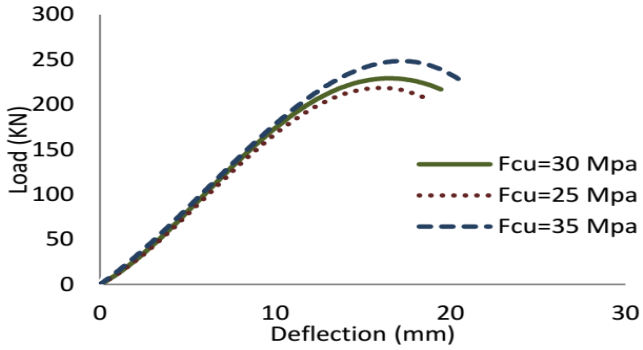

Fig. 23. Load- Def comparison depended on concrete compressive strength for S0.

Table 7. Numerical models characteristics

Slab Code	Fcu (Mpa)	Load Condition	Punching Shear Rft. or strengthening		
			Applied Material	Distance Between Stirrups (mm)	Width of Stirrups (mm)
SSE1	30	Eccentric e/t=0.4	Steel Stirrups	30	140
SGE1	30		GFRPS	30	
SCE1	30			30	
SCE2	30		CFRPS	50	
SCE3	30			60	
SE0.4	30		-	-	-
SE0.8	30	Eccentric e/t=0.8	-	-	-
S030	30	Centric load e/t=0	-	-	-
S025	25		-	-	-
S035	35		-	-	-

7. Conclusion

In this research, steel and FRPS were used to increase flat slab punching shear capacities against failure. FRPS were fixed surrounding the column beginning from (d/4) from the column face of F-S. A total of six flat slabs were established and tested up to failure, one reference specimen without reinforcing, two specimens reinforced by steel stirrups of 140 mm width, two specimens reinforced using GFRPS with 140 mm width, the first five specimens subjected to eccentric load and the last specimen subjected to centric load. The test variables for the reinforcing approaches under consideration were the reinforcement material type, the distance between stirrups, and the load case. The following conclusions can be summarized based on this investigation:

1. The punching shear behaviour of R-C-F-S was improved by utilizing stirrups as reinforcement. The reference specimen (zero% punching reinforcement) collapsed in a brittle punching failure mode, whereas cracks were spread over a wider distance.
2. There has been a significant increase in the final punching strength for reinforced specimens. When compared to the reference specimen, the punching capacity rose for specimens reinforced with steel stirrups by 28 - 41% and for specimens reinforced with GFRPS by 43 - 63 percent.
3. The specimens reinforced with steel stirrups and spaced 50 mm apart from one another proved a considerable increase in punching capacity of 10 % over specimens spaced 70 mm apart. Also, the punching capacity of specimens reinforced by GFRPS with a distance of 50 mm between each one increased significantly by 14% compared to the specimens with a distance of 70 mm.
4. Specimens reinforced by stirrups demonstrated significantly improved def capacity and ductility in addition to a major improvement in punching capacity. This growth might be important because it provides an observant warning before the punching failure.
5. All reinforced specimens had stiffnesses that ranged from 32% to 57% greater than the control specimen in the uncracked stage. Reinforcement material had an impact on the stiffness at the cracked stage. Whereas, for specimens reinforced by punching shear stirrups, the ultimate stiffness was enhanced by 14 to 26% as compared to the control specimen.
6. Punching failure mode caused the collapse of all flat slabs. Compared to the control F-S, the F-S reinforced by stirrups showed a higher punching capacity.
7. The punching capacity of the F-S significantly increased when the number of stirrups was increased (the distance between stirrups was decreased).
8. Using various materials to fabricate the stirrups used in the punching reinforcement has improved the punching strength of the slabs. the punching strength of specimens reinforced with GFRPS was enhanced compared to specimens reinforced by steel stirrups.

9. There is a significant agreement between the calculated punching shear capacity using recently created analytical models FE of all the tested specimens and the experimental results, with an average agreement of 0.95 and a standard deviation of 0.024. The computed punching strengths of all the studied specimens using a recently created analytical model on Abaqus/CAE6.14 are well-concordant with the experimental data by an average of 1.058 and standard deviation of 0.008.

References

[1] G. T. Truong, K. K. Choi, and C. S. Kirr, "Punching Shear Strength of Interior Concrete Slab-Column Connections Reinforced with FRP Flexural and Shear Reinforcement," Journal of Building Engineering, ElSEVIER, vol. 46, no. 1, pp.103692, Apr., 2022.

[2] B. Wieczorek, "Numerical Analysis of the Inner Slab–Column Connection of RC Structures Loaded Eccentrically," Science Direct, ElSEVIER, vol. 172, 1110 – 1114, 2017.

[3] K. Sissakis, and S. A. Sheikn, "Strengthening Concrete Slabs for Punching Shear with Carbon Fiber-Reinforced Polymer Laminates," Aci Structural Journal, vol. 104, no. 1, pp.104-S06, Apr., 2007.

[4] C. Aksoylu, "Experimental analysis of shear deficient reinforced concrete beams strengthened by glass fiber strip composites and mechanical stitches," Compos Struct, Techno Press, vol. 40, no. 2, pp. 267-285, Jul., 2021.

[5] Y. O. Özkılıç, Ş. Yazman, C. Aksoylu, M. H. Arslan, and L. Gemi, "Numerical investigation of the parameters influencing the behavior of dapped end prefabricated concrete purlins with and without CFRP strengthening," Constr. Build, Mater, vol. 275, no. 15, pp. 10.1016, Mar., 2021.

[6] L. Gemi, C. Aksoylu, Ş. Yazman, Y. O. Özkılıç, and M. H. Arslan, "Experimental investigation of shear capacity and damage analysis of thinned end prefabricated concrete purlins strengthened by CFRP," Compos Struct, ElSEVIER, vol. 229, no. 1, pp. 111399, Dec., 2019.

[7] C. Aksoylu, Ş. Yazman, Y. O. Özkılıç, L. Gemi, and M. H. Arslan, "Experimental analysis of reinforced concrete shear deficient beams with circular web openings strengthened by CFRP," Compos Struct, ElSEVIER, vol. 249, no. 1, pp. 112561, Oct., 2020.

[8] A. Deifalla, A. Awad, and M. El-Garhy, "Effectiveness of externally bonded CFRP strips for strengthening flanged beams under torsion an experimental study," Eng. Struct, vol. 56, pp. 2065-2075, 2013.

[9] L. Gemi, M. A. Köroğlu, and A. Ashour, "Experimental study on compressive behaviour and failure analysis of composite concrete confined by glass/epoxy ±55° filament wound pipes," Compos Struct, ElSEVIER, vol. 187, no. 1, pp. 157-168, Mar., 2018.

[10] A. Saribiyik, B. Abodan, and M. T. Balci, "Experimental study on shear strengthening of RC beams with basalt RP strips using different wrapping methods," Eng. Sci. Technol. Int. J., ElSEVIER, vol. 24, no. 1, pp. 192-204, Mar., 2021.

[11] M. Gediminas, and S. Remigijus, "Calculation of punching shear strength of steel fiber reinforced concrete flat slabs," Science Direct, ElSEVIER, vol. 172, 1110 – 1114, 2017.

[12] K. Soudki, A. K. El-Sayed, and T. Vanzwol, "Strengthening of Concrete Slab-Column Connections Using CFRP Strips," Journal of King Saud University, Engineering Sciences, vol. 24, no. 1, pp.25-33, Aug., 2012.

[13] G. I. Khalil, "New Punching Shear Strengthening Technique for Concrete Slab-Column Connections Using FRP,", https://bu.edu.eg/staff/gamalismail-publications/18163, 2004.

[14] M. H. Makhlouf, G. I. Khalil, I. G. Shaaban, and K. M. Elsayed "Strengthening of Reinforced Concrete Slab-Column Connection Subjected to Punching Shear with FRP Systems," IACSIT International Journal of Engineering and Technology, vol. 5, no. 6, Dec., 2013.

[15] M. H. Makhlouf *, G. Ismail, A. H. Abdel Kreem, M. I. Badawi, "Investigation of transverse reinforcement for R.C flat slabs against punching shear and comparison with innovative strengthening technique using FRP ropes", ELSEVIER, Case Studies in Construction Materials, vol. 18, Feb., 2023.

[16] I. El-Sayed, and M. Ismail, "Non-linear finite element analysis of reinforced concrete flat plates with opening adjacent to column under eccentric punching loads," HBRC Journal, ElSEVIER, 1687-4048, 2018.

[17] A. E. Salama, M. Hassan, and B. Benmokrane, "Effectiveness of Glass Fiber-Reinforced Polymer Stirrups as Shear Reinforcement in Glass Fiber-Reinforced Polymer-Reinforced Concrete Edge Slab-Column Connections," Aci Structural Journal, Technical Paper, no. 116-S105, Sep., 2019.

[18] D. L. Tan, et al., "A rational formula to predict punching shear capacity at interior columns connections with RC flat slabs reinforced with either steel or FRP bars but without shear reinforcement," Construction and Building Materials, ElSEVIER, vol. 248, no. 10, pp. 118362, Jul., 2020.

[19] T. D. Dai, et al., "Efficacy of CFRP/BFRP laminates in flexural strengthening of concrete beams with corroded reinforcement," Journal of Building Engineering, ElSEVIER, vol. 53, no. 1, pp. 104606, Aug., 2022.

[20] B. Benmokrane, E. El-Salakawy, S. El-Gamal, S. and Goulet, "Construction and Testing of an Innovative Concrete Bridge Deck Totally Reinforced with Glass FRP Bars: Val-Alain Bridge on Highway 20 East," Journal of Bridge Engineering, ASCE, vol. 12, no. 5, pp. 632-645, 2007.

[21] M. El-Gendy, and E. El-Salakawy, “Effect of Shear Studs and High Moments on Punching Behavior of GFRP-RC Slab-Column Edge Connections,” Journal of Composites for Construction, ASCE, vol. 20, no. 4., 2016.

[22] A. Mostafa, and E. El-Salakawy, “Behavior of GFRP-RC Slab-Column Edge Connections with High-Strength Concrete and Shear Rein¬forcement,” Journal of Composites for Construction, ASCE, vol. 22, no. 2, 2018.

[23] A. Gouda, and E.El-Salakawy, “Punching Shear Strength of GFRP-RC Interior Slab-Column Connections Subjected to Moment Transfer,” Journal of Composites for Construction, ASCE, vol. 20, no. 1, Feb., 2015.

[24] X. Fan, S. Gu, X. Wu, and J. Jiang, “Critical shear crack theory-based punching shear model for FRP-reinforced concrete slabs,” Advances in Structural Engineering, ElSEVIER, vol. 24, no. 6, pp. 1208–1220, Dec. 2020.

[25] E. Oller, R. Kotynia, and A. Marí, “Assessment of the existing formulations to evaluate shear-punching strength in RC slabs with FRP bars without transverse reinforcement,” High Tech Concrete, Springer, 2018.

[26] A. Deifalla, “Punching shear strength and deformation for FRP-reinforced concrete slabs without shear reinforcements,” Case Studies in Construction Materials, ElSEVIER, vol.16, pp. e00925, Nov., 2022.

[27] ACI Committee 318, “Building Code Requirements for Structural Concrete (ACI 318-14) and Commentary (ACI 318R-14),” American Concrete Institute, Farmington Hills, MI, 520 pp, 2014.

[28] ACI Committee 440, “Guide Test Methods for Fiber-Reinforced Polymers (FRPs) for Reinforcing or Strengthening Concrete Structures (ACI 440.3R-12),” American Concrete Institute, Farmington Hills, MI, 23 pp, 2012.

[29] ACI Committee 440, “Guide for the Design and Construction of Concrete Reinforced with FRP Bars (ACI 440.1R-15),” American Concrete Institute, Farmington Hills, MI, 88 pp, 2015.

[30] ACI Committee 421, “Guide to Shear Reinforcement for Slabs (ACI 421.1R-08)”, American Concrete Institute, Farmington Hills, MI, 48331, 2008.

[31] A. H. Ali, A. Gouda, and H. R. Mohamed, “Nonlinear finite elements modelling and experiments of FRP-reinforced concrete piles under shear loads,” Structures, ElSEVIER, vol. 106, no. 119., Aug. 2020.

[32] R. T. S. Mabrouk, G. S. Younis, and O. M. Ramadan, “Experimental Evaluation of the Punching Shear Strength of Interior Slab-Column Connection with Different Shear Reinforcement Details,” Civil Engineering Journal, C.E.J, vol. 8, no. 09, E-ISSN: 2476-3055, Sep., 2022.